Series solutions of unsteady free convection flow in the stagnation-point region of a three-dimensional body

Hang Xu [a], Shi-Jun Liao [a,*], Ioan Pop [b]

[a] *State Key Lab of Ocean Engineering, School of Naval Architecture, Ocean and Civil Engineering, Shanghai Jiao Tong University, Shanghai 200030, China*
[b] *Faculty of Mathematics, University of Cluj, R-3400 Cluj, CP253, Romania*

Abstract

The unsteady three-dimensional free convection flow in the stagnation-point region on a general curved isothermal surface placed in an ambient fluid is studied. By introducing new similarity transformations, the momentum and energy balance equations are reduced to a set of three fully coupled nonlinear partial differential equations. These equations are solved analytically for some various values of the ratio of the two principal radii of curvature. The accurate series solutions are obtained which are uniformly valid for all dimensionless time in the whole spatial region $0 \leqslant \eta < \infty$.

© 2007 Elsevier Masson SAS. All rights reserved.

Keywords: Free convection; Stagnation point; Unsteady; Boundary-layer; Series solution

1. Introduction

The phenomenon of free convection will be happened when a surface or body in a fluid is sudden heated. The reason is that the sudden temperature changes of the surface cause density variations leading to buoyancy forces. This process of heat transfer is encountered in the natural environment such as in atmosphere and oceanic circulations and in technology such as in power transformers, nuclear reactor, etc. Several excellent review papers of the literature related to the free convection flows are presented by Ede [1], Gebhart [2] and Gebhart et al. [3]. Poots [4] investigated steady three dimensional steady free convection near the lower stagnation point on an isothermal curved surface. Banks [5] extended the calculations of Poots [4] to negative values of *c* corresponding to saddle points of attachment. Williams et al. [6] investigated the unsteady free convection flow over a vertical flat plate under the assumption that the wall temperature varies with time and distance and found possible semi-similar solutions for a variety of classes of wall temper-

ature distributions. Takhar et al. [7] studied the unsteady free convection boundary-layer flow in the forward stagnation-point region of a sphere with time-dependent angular velocity in an ambient fluid. Slaouti et al. [8] made an analysis on the unsteady free convection flow in the stagnation-point region of a heated three-dimensional body placed in an ambient fluid. All of these kinds of problems are studied, theoretically, numerically or experimentally, by many researchers such as Merkin [9], Carey [10], Merkin and Mahmood [11], Kumari et al. [12], Miyamoto [13], Soundalgekar and Ganesan [14], Cheng [15], Aziz and Hellums [16], Banks [17], Suwono [18], Xu [19], Wang [20].

The homotopy analysis method (HAM) [21–24] is an powerful analytical tool for nonlinear problems. It has been accepted by more and more researchers, and many of their work [25–40] have been appeared in various fields. Unlike perturbation techniques, it is independent of any small physical parameters at all. Different from all previous analytic methods, the homotopy analysis method provides us with a simple way to ensure the convergence of the solution series, so that we can always get accurate enough approximations. Currently, it is pointed out [25–28] that the so-called "homotopy perturbation method" [41] proposed in 1999 is only a special case of the homotopy analysis method propounded in 1992 [21,22]. All of these ver-

ify the generality and validity of the homotopy analysis method for nonlinear problems.

The object of this paper is to extend the work of Poots [4] to the unsteady case. By means of new similarity transformations, the original momentum and energy balance equations are reduced to a set of three fully coupled nonlinear partial differential equations. It is convenient to choose time scale ξ so that the region of time integration $0 \leqslant t < \infty$ becomes finite, $0 \leqslant \xi \leqslant 1$. Note that this transformation may reduce the calculation quantities, thus the convergent results may be recovered more easier. The homotopy analysis method will then be employed to solve this problem. By introducing an embedding parameter q the nonlinear ordinary differential equation is converted to a linear differential equation at $q = 0$. When q evolves, the differential equation becomes the original one at $q = 1$. This technique has been used in a variety of nonlinear problems and the details can be found in Liao [22]. It is the first time that the homotopy analysis method [22] is applied to study the unsteady free convection and heat transfer phenomena, to the best of our knowledge.

2. Mathematical description

Consider the unsteady free convection boundary-layer flow in the stagnation-point region of a heated three-dimensional body placed in an ambient fluid. It is assumed that at time $t = 0$, the three-dimensional body and the fluid are at rest and they have the same constant temperature T_∞. Then at time $t = 0$, the surface temperature of the body is raised from T_∞ to the constant value T_w, where $T_w > T_\infty$. Under these conditions the governing equations for the unsteady boundary layer flow and heat transfer for this problem are

$$\frac{\partial u}{\partial x} + \frac{\partial v}{\partial y} + \frac{\partial w}{\partial z} = 0 \tag{1}$$

$$\frac{\partial u}{\partial t} + u\frac{\partial u}{\partial x} + v\frac{\partial u}{\partial y} + w\frac{\partial u}{\partial z} - g\beta ax(T - T_\infty) = \nu\frac{\partial^2 u}{\partial z^2} \tag{2}$$

$$\frac{\partial v}{\partial t} + u\frac{\partial v}{\partial x} + v\frac{\partial v}{\partial y} + w\frac{\partial v}{\partial z} - g\beta by(T - T_\infty) = \nu\frac{\partial^2 v}{\partial z^2} \tag{3}$$

$$\frac{\partial T}{\partial t} + u\frac{\partial T}{\partial x} + v\frac{\partial T}{\partial y} + w\frac{\partial T}{\partial z} = \alpha\frac{\partial^2 T}{\partial z^2} \tag{4}$$

where u, v and w are the velocity components in the x-, y- and z-directions, t denotes the time, ρ, β, ν and α are, respectively, the density, the bulk coefficient of the thermal expansion, kinematic viscosity of the fluid and the thermal diffusivity of the fluid. a and b are the principal curvatures of the body at the stagnation point. The corresponding initial and boundary conditions are

$$t < 0: \quad u = v = w = 0, \quad T = T_\infty \tag{5a}$$

$$t \geqslant 0: \quad u = 0, \quad v = 0, \quad w = 0, \quad T = T_w \quad \text{at } z = 0 \tag{5b}$$

$$t \geqslant 0: \quad u \to 0, \quad v \to 0, \quad T \to 0 \quad \text{as } z \to +\infty \tag{5c}$$

Following Williams and Rhyne [42], we introduce the new similarity transformations

$$\eta = Gr^{\frac{1}{4}}a\frac{z}{\sqrt{\xi}}, \quad \xi = 1 - \exp(-\tau), \quad \tau = \nu a^2 Gr^{\frac{1}{2}}t$$

$$u = \nu a^2 x\, Gr^{\frac{1}{2}}\frac{\partial F}{\partial \eta}, \qquad v = \nu a^2 cy\, Gr^{\frac{1}{2}}\frac{\partial S}{\partial \eta}$$

$$w = -\nu a\xi^{\frac{1}{2}}Gr^{\frac{1}{4}}(F + cS), \qquad G = \frac{T - T_\infty}{T_w - T_\infty} \tag{6}$$

where $Gr = g\beta(T_w - T_\infty)/(a^3\nu^2)$ is the Grashof number.

Substituting (6) into Eqs. (1)–(4), we have

$$(1 - \xi)\left(\xi\frac{\partial^2 F}{\partial\eta\partial\xi} - \frac{\eta}{2}\frac{\partial^2 F}{\partial\eta^2}\right)$$
$$- \xi\left[(F + cS)\frac{\partial^2 F}{\partial\eta^2} + G - \left(\frac{\partial F}{\partial\eta}\right)^2\right] - \frac{\partial^3 F}{\partial\eta^3} = 0 \tag{7}$$

$$(1 - \xi)\left(\xi\frac{\partial^2 S}{\partial\eta\partial\xi} - \frac{\eta}{2}\frac{\partial^2 S}{\partial\eta^2}\right)$$
$$- \xi\left[(F + cS)\frac{\partial^2 S}{\partial\eta^2} + cG - c\left(\frac{\partial S}{\partial\eta}\right)^2\right] - \frac{\partial^3 S}{\partial\eta^3} = 0 \tag{8}$$

$$(1 - \xi)\left(\xi\frac{\partial G}{\partial\xi} - \frac{\eta}{2}\frac{\partial G}{\partial\eta}\right) - \xi(F + cS)\frac{\partial G}{\partial\eta}$$
$$- Pr^{-1}\frac{\partial^2 G}{\partial\eta^2} = 0 \tag{9}$$

subject to the boundary conditions

$$F(0, \xi) = S(0, \xi) = \left.\frac{\partial F(\eta, \xi)}{\partial\eta}\right|_{\eta=0} = \left.\frac{\partial S(\eta, \xi)}{\partial\eta}\right|_{\eta=0} = 0$$

$$G(0, \xi) = 1$$

$$\left.\frac{\partial F(\eta, \xi)}{\partial\eta}\right|_{\eta\to+\infty} = \left.\frac{\partial S(\eta, \xi)}{\partial\eta}\right|_{\eta\to+\infty} = G(+\infty, \xi) = 0 \tag{10}$$

where $c = b/a$ is a positive constant, $Pr = \nu/\alpha$ is the Prandtl number. We shall only consider the case $0 \leqslant c \leqslant 1$ since most shapes of practical interest lie between cylinder ($c = 0$) and sphere ($c = 1$). In this case, both a and b are positive, thus solutions of the resulting equations lead to stagnation points which are nodal points. However a or b could also be negative which leads to saddle points of attachment $-1 \leqslant c \leqslant 0$. A more detailed analysis for this physical model can be found in [8].

When $\xi = 0$, corresponding to $\tau = 0$, we have from (7), (8) and (9) that

$$\frac{\partial^3 F}{\partial\eta^3} + \frac{\eta}{2}\frac{\partial^2 F}{\partial\eta^2} = 0 \tag{11}$$

$$\frac{\partial^3 S}{\partial\eta^3} + \frac{\eta}{2}\frac{\partial^2 S}{\partial\eta^2} = 0 \tag{12}$$

$$\frac{1}{Pr}\frac{\partial^2 G}{\partial\eta^2} + \frac{\eta}{2}\frac{\partial G}{\partial\eta} = 0 \tag{13}$$

subject to the boundary conditions

$$F(0, 0) = S(0, 0) = \left.\frac{\partial F(\eta, \xi)}{\partial\eta}\right|_{\eta=0,\,\xi=0}$$

$$= \left.\frac{\partial S(\eta, \xi)}{\partial\eta}\right|_{\eta=0,\,\xi=0} = 0$$

$$G(0, 0) = 1$$

$$\left.\frac{\partial F(\eta,\xi)}{\partial \eta}\right|_{\eta\to+\infty,\ \xi=0} = \left.\frac{\partial S(\eta,\xi)}{\partial \eta}\right|_{\eta\to+\infty,\ \xi=0}$$
$$= G(+\infty,0) = 0 \qquad (14)$$

The above equations (11), (12) and (13) have the exact solutions

$$F(\eta,0) = S(\eta,0) = 0, \qquad G(\eta,0) = \mathrm{erfc}\left(\frac{\sqrt{Pr}\,\eta}{2}\right) \qquad (15)$$

where

$$\mathrm{erfc}(\eta) = 1 - \frac{2}{\sqrt{\pi}}\int_0^\eta \exp(-x^2)\,\mathrm{d}x \qquad (16)$$

When $\xi = 1$, corresponding to $\tau \to +\infty$, we have

$$\frac{\partial^3 F}{\partial \eta^3} + (F+cS)\frac{\partial^2 F}{\partial \eta^2} + G - \left(\frac{\partial F}{\partial \eta}\right)^2 = 0 \qquad (17)$$

$$\frac{\partial^3 S}{\partial \eta^3} + (F+cS)\frac{\partial^2 S}{\partial \eta^2} + cG - c\left(\frac{\partial S}{\partial \eta}\right)^2 = 0 \qquad (18)$$

$$Pr^{-1}\frac{\partial^2 G}{\partial \eta^2} + (F+cS)\frac{\partial G}{\partial \eta} = 0 \qquad (19)$$

subject to the boundary conditions

$$F(0,1) = S(0,1) = \left.\frac{\partial F(\eta,\xi)}{\partial \eta}\right|_{\eta=0,\ \xi=1}$$
$$= \left.\frac{\partial S(\eta,\xi)}{\partial \eta}\right|_{\eta=0,\ \xi=1} = 0$$
$$G(0,1) = 1$$

$$\left.\frac{\partial F(\eta,\xi)}{\partial \eta}\right|_{\eta\to+\infty,\ \xi=1} = \left.\frac{\partial S(\eta,\xi)}{\partial \eta}\right|_{\eta\to+\infty,\ \xi=1}$$
$$= G(+\infty,1) = 0 \qquad (20)$$

The quantities of physical interest in this problem are the local skin friction coefficients, C_{fx} and C_{fy}, and the local Nusselt number, Nu, which can be expressed as

$$C_{fx}/(Gr)^{3/4} = \frac{1}{\sqrt{\xi}}\frac{\partial^2 F(\xi,0)}{\partial \eta^2}$$

$$C_{fy}/(Gr)^{3/4} = \frac{c}{\sqrt{\xi}}\frac{\partial^2 S(\xi,0)}{\partial \eta^2}$$

$$Nu/(Gr)^{1/4} = \frac{1}{\sqrt{\xi}}\frac{\partial G(\xi,0)}{\partial \eta} \qquad (21)$$

3. Homotopy analysis solution

3.1. HAM deformation equations

According to boundary conditions (10), it is nature that $F(\eta,\xi)$, $S(\eta,\xi)$ and $G(\eta,\xi)$ can be expressed by the function

$$\{\xi^k \eta^m \exp(-n\eta) \mid k \geqslant 0,\ n \geqslant 0,\ m \geqslant 0\} \qquad (22)$$

in the following form

$$F(\eta,\xi) = \sum_{k=0}^{+\infty}\sum_{m=0}^{+\infty}\sum_{n=1}^{+\infty} a_{m,n}^k \xi^k \eta^m \exp(-n\eta) \qquad (23a)$$

$$S(\eta,\xi) = \sum_{k=0}^{+\infty}\sum_{m=0}^{+\infty}\sum_{n=1}^{+\infty} b_{m,n}^k \xi^k \eta^m \exp(-n\eta) \qquad (23b)$$

$$G(\eta,\xi) = \sum_{k=0}^{+\infty}\sum_{m=0}^{+\infty}\sum_{n=1}^{+\infty} c_{m,n}^k \xi^k \eta^m \exp(-n\eta) \qquad (23c)$$

where $a_{m,n}^k$, $b_{m,n}^k$ and $c_{m,n}^k$ are coefficients. These provide us with the *Solution Expressions* for $F(\eta,\xi)$, $S(\eta,\xi)$ and $G(\eta,\xi)$. According to the *Solution Expressions* (23a)–(23c) and from the boundary conditions (10), it is convenient to choose

$$F_0(\eta,\xi) = S_0(\eta,\xi) = 0, \qquad G_0(\eta,\xi) = \exp(-\eta) \qquad (24a)$$

as the initial approximations of $F(\eta,\xi)$, $S(\eta,\xi)$ and $G(\eta,\xi)$, besides to choose

$$\mathcal{L}_f\big[\Phi(\xi,\eta;q)\big] = \frac{\partial^3 \Phi}{\partial \eta^3} - \frac{\partial \Phi}{\partial \eta} \qquad (25a)$$

$$\mathcal{L}_s\big[\Theta(\xi,\eta;q)\big] = \frac{\partial^3 \Theta}{\partial \eta^3} - \frac{\partial \Theta}{\partial \eta} \qquad (25b)$$

$$\mathcal{L}_g\big[\Psi(\xi,\eta;q)\big] = \frac{\partial^2 \Psi}{\partial \eta^2} - \Psi \qquad (25c)$$

as the auxiliary linear operators, which have the following properties

$$\mathcal{L}_f\big[C_1\exp(-\eta) + C_2\exp(\eta) + C_3\big] = 0 \qquad (26a)$$

$$\mathcal{L}_s\big[C_4\exp(-\eta) + C_5\exp(\eta) + C_6\big] = 0 \qquad (26b)$$

$$\mathcal{L}_g\big[C_7\exp(-\eta) + C_8\exp(\eta)\big] = 0 \qquad (26c)$$

where C_1, C_2, C_3, C_4, C_5, C_6, C_7 and C_8 are constants. Based on (7), (8) and (9), we are led to define the nonlinear operators

$$\mathcal{N}_f\big[\Phi(\eta,\xi;q)\big] = (1-\xi)\left(\frac{\eta}{2}\frac{\partial^2 \Phi}{\partial \eta^2} - \xi\frac{\partial^2 \Phi}{\partial \eta \partial \xi}\right) + \frac{\partial^3 \Phi}{\partial \eta^3}$$
$$+ \xi\left[(\Phi + c\Theta)\frac{\partial^2 \Phi}{\partial \eta^2} + \Psi - \left(\frac{\partial \Phi}{\partial \eta}\right)^2\right] \qquad (27a)$$

$$\mathcal{N}_s\big[\Theta(\eta,\xi;q)\big] = (1-\xi)\left(\frac{\eta}{2}\frac{\partial^2 \Theta}{\partial \eta^2} - \xi\frac{\partial^2 \Theta}{\partial \eta \partial \xi}\right) + \frac{\partial^3 \Theta}{\partial \eta^3}$$
$$+ \xi\left[(\Phi + c\Theta)\frac{\partial^2 \Theta}{\partial \eta^2} + c\Psi - c\left(\frac{\partial \Theta}{\partial \eta}\right)^2\right] \qquad (27b)$$

$$\mathcal{N}_g\big[\Psi(\eta,\xi;q)\big] = (1-\xi)\left(\frac{\eta}{2}\frac{\partial \Psi}{\partial \eta} - \xi\frac{\partial \Psi}{\partial \xi}\right) + \frac{1}{Pr}\frac{\partial^2 \Psi}{\partial \eta^2}$$
$$+ \xi(\Phi + c\Theta)\frac{\partial \Psi}{\partial \eta} \qquad (27c)$$

Let $\hbar$ denote the non-zero auxiliary parameters. We construct the so-called zeroth-order deformation equations

$$(1-q)\mathcal{L}_f\big[\Phi(\eta,\xi;q)-f_0(\eta,\xi)\big]$$
$$= q\hbar H(\eta)\mathcal{N}_f\big[\Phi(\eta,\xi;q)\big] \tag{28a}$$

$$(1-q)\mathcal{L}_s\big[\Theta(\eta,\xi;q)-s_0(\eta,\xi)\big]$$
$$= q\hbar H(\eta)\mathcal{N}_s\big[\Theta(\eta,\xi;q)\big] \tag{28b}$$

$$(1-q)\mathcal{L}_g\big[\Psi(\eta,\xi;q)-g_0(\eta,\xi)\big]$$
$$= q\hbar H(\eta)\mathcal{N}_g\big[\Psi(\eta,\xi;q)\big] \tag{28c}$$

subject to the boundary conditions

$$\Phi(0,\xi)=\Theta(0,\xi)=\frac{\partial\Phi(\eta,\xi)}{\partial\eta}\bigg|_{\eta=0}=\frac{\partial\Theta(\eta,\xi)}{\partial\eta}\bigg|_{\eta=0}=0$$

$$\Psi(0,\xi)=1$$

$$\frac{\partial\Phi(\eta,\xi)}{\partial\eta}\bigg|_{\eta\to+\infty}=\frac{\partial\Theta(\eta,\xi)}{\partial\eta}\bigg|_{\eta\to+\infty}=\Psi(+\infty,\xi)=0 \tag{29}$$

where $q\in[0,1]$ is an embedding parameter, $H(\eta)=\exp(-\eta)$ is an auxiliary function.

Obviously, when $q=0$ and $q=1$, the above HAM deformation equations (28a)–(28c) have the solutions

$$\Phi(\eta,\xi;0)=F_0(\eta,\xi),\qquad \Theta(\eta,\xi;0)=S_0(\eta,\xi)$$
$$\Psi(\eta,\xi;0)=G_0(\eta,\xi) \tag{30a}$$

and

$$\Phi(\eta,\xi;1)=F(\eta,\xi),\qquad \Theta(\eta,\xi;1)=S(\eta,\xi)$$
$$\Psi(\eta,\xi;1)=G(\eta,\xi) \tag{30b}$$

respectively. Thus as q increases from 0 to 1, $\Phi(\eta,\xi;q)$, $\Theta(\eta,\xi;q)$ and $\Psi(\eta,\xi;q)$ vary from the initial guesses $F_0(\eta,\xi)$, $S_0(\eta,\xi)$ and $G_0(\eta,\xi)$ to the solutions $F(\eta,\xi)$, $S(\eta,\xi)$ and $G(\eta,\xi)$ of the considered unsteady problem, respectively. So, expanding $\Phi(\eta,\xi;q)$, $\Theta(\eta,\xi;q)$ and $\Psi(\eta,\xi;q)$ in Taylor's series with respect to q, we have

$$\Phi(\eta,\xi;q)=\Phi(\eta,\xi,0)+\sum_{m=1}^{+\infty}F_m(\eta,\xi)q^m \tag{31a}$$

$$\Theta(\eta,\xi;q)=\Theta(\eta,\xi,0)+\sum_{m=1}^{+\infty}S_m(\eta,\xi)q^m \tag{31b}$$

$$\Psi(\eta,\xi;q)=\Psi(\eta,\xi,0)+\sum_{m=1}^{+\infty}G_m(\eta,\xi)q^m \tag{31c}$$

where

$$F_m(\eta,\xi)=\frac{1}{m!}\frac{\partial^m\Phi(\eta,\xi;q)}{\partial q^m}\bigg|_{q=0} \tag{32a}$$

$$S_m(\eta,\xi)=\frac{1}{m!}\frac{\partial^m\Theta(\eta,\xi;q)}{\partial q^m}\bigg|_{q=0} \tag{32b}$$

$$G_m(\eta,\xi)=\frac{1}{m!}\frac{\partial^m\Psi(\eta,\xi;q)}{\partial q^m}\bigg|_{q=0} \tag{32c}$$

Note that (28a), (28b) and (28c) contain the auxiliary parameter $\hbar$. Assuming that $\hbar$ is properly chosen so that the series (31a)–(31c) are convergent at $q=1$, we have, using (30a) and (30b), the solution series

$$F(\eta,\xi)=F_0(\eta,\xi)+\sum_{m=1}^{+\infty}F_m(\eta,\xi) \tag{33a}$$

$$S(\eta,\xi)=S_0(\eta,\xi)+\sum_{m=1}^{+\infty}S_m(\eta,\xi) \tag{33b}$$

$$G(\eta,\xi)=G_0(\eta,\xi)+\sum_{m=1}^{+\infty}G_m(\eta,\xi) \tag{33c}$$

3.2. High-order deformation equation

For simplicity, we define the vector

$$\vec{F}_m=\{F_0,F_1,\ldots,F_m\},\qquad \vec{S}_m=\{S_0,S_1,\ldots,S_m\},$$
$$\vec{G}_m=\{G_0,G_1,\ldots,G_m\} \tag{34}$$

Differentiating the zeroth-order deformation equations (28a)–(28c) m times with respect to q, then setting $q=0$, and finally dividing them by $m!$, we obtain the mth-order deformation equations

$$\mathcal{L}_f\big[F_m(\eta,\xi)-\chi_m F_{m-1}(\eta,\xi)\big]=\hbar R_m(\vec{F}_{m-1}) \tag{35a}$$

$$\mathcal{L}_s\big[S_m(\eta,\xi)-\chi_m S_{m-1}(\eta,\xi)\big]=\hbar S_m(\vec{S}_{m-1}) \tag{35b}$$

$$\mathcal{L}_g\big[G_m(\eta,\xi)-\chi_m G_{m-1}(\eta,\xi)\big]=\hbar W_m(\vec{G}_{m-1}) \tag{35c}$$

subject to the boundary conditions

$$F_m(0,\xi)=S_m(0,\xi)=G_m(0,\xi)=\frac{\partial F_m(\eta,\xi)}{\partial\eta}\bigg|_{\eta=0}$$

$$=\frac{\partial S_m(\eta,\xi)}{\partial\eta}\bigg|_{\eta=0}=0$$

$$G_m(\infty,\xi)=\frac{\partial F_m(\eta,\xi)}{\partial\eta}\bigg|_{\eta\to+\infty}=\frac{\partial S_m(\eta,\xi)}{\partial\eta}\bigg|_{\eta\to+\infty}=0 \tag{36}$$

where

$$R_m(\vec{F}_{m-1})=\frac{1}{(m-1)!}\frac{\partial^{m-1}\mathcal{N}_f[\Phi(\eta,\xi;q)]}{\partial q^{m-1}}\bigg|_{q=0} \tag{37a}$$

$$S_m(\vec{S}_{m-1})=\frac{1}{(m-1)!}\frac{\partial^{m-1}\mathcal{N}_s[\Theta(\eta,\xi;q)]}{\partial q^{m-1}}\bigg|_{q=0} \tag{37b}$$

$$W_m(\vec{G}_{m-1})=\frac{1}{(m-1)!}\frac{\partial^{m-1}\mathcal{N}_g[\Psi(\eta,\xi;q)]}{\partial q^{m-1}}\bigg|_{q=0} \tag{37c}$$

and

$$\chi_m=\begin{cases}0,&m=1\\1,&m>1\end{cases} \tag{38}$$

Let $F_m^*(\eta,\xi)$, $S_m^*(\eta,\xi)$ and $G_m^*(\eta,\xi)$ denote the particular solutions of (35a)–(35c). Using (26a)–(26c), we have the general solutions

$$F_m(\eta,\xi)=F_m^*(\eta,\xi)+C_1^m\exp(-\eta)$$
$$+C_2^m\exp(\eta)+C_3^m \tag{39a}$$

$$S_m(\eta,\xi)=S_m^*(\eta,\xi)+C_4^m\exp(-\eta)$$
$$+C_5^m\exp(\eta)+C_6^m \tag{39b}$$

$$g_m(\eta,\xi)=G_m^*(\eta,\xi)+C_7^m\exp(-\eta)+C_8^m\exp(\eta) \tag{39c}$$

where the coefficients C_1^m, C_2^m, C_3^m, C_4^m, C_5^m, C_6^m, C_7^m and C_8^m are determined by the boundary conditions (36), i.e.

$$C_2^m = C_5^m = C_8^m = 0, \qquad C_1^m = \left.\frac{\partial F_m^*(\eta, \xi)}{\partial \eta}\right|_{\eta=0}$$

$$C_3^m = -C_1^m - F_m^*(0, \xi), \qquad C_4^m = \left.\frac{\partial S_m^*(\eta, \xi)}{\partial \eta}\right|_{\eta=0}$$

$$C_6^m = -C_4^m - S_m^*(0, \xi), \qquad C_7^m = -G_m^*(0, \xi) \tag{40}$$

In this way, it is easy to solve the *linear* equations (35a)–(35c) after the other in the order $m = 1, 2, 3, \ldots$ by means of the symbolic computation software such as Mathematica, Maple.

4. Analysis of results

Liao [22] proved in general that, as long as a solution series given by the homotopy analysis method is not divergent, it must converge to the exact solution of nonlinear problems under investigation. Note that the solution series (33a)–(33c) contain the auxiliary parameter $\hbar$, which influences the convergence of the series (33a)–(33c). Thus, mathematically, the series solutions are dependent upon $\hbar$. But, physically, the solution should be independent of the auxiliary parameter $\hbar$. As a result, the HAM series must converge to the *same* result for all corresponding values of $\hbar$ which ensures the convergence. For example, given c and Pr, the series of $F''(0, 0)$ converges to the *same* value, for *all* possible values of auxiliary parameter $\hbar$ which ensures the convergence of the series. So, if one regards $\hbar$ as a variable and plots the curve $F''(0, 0) \sim \hbar$, one would find a line segment parallel to the horizontal axis: all values of $\hbar$ below this parallel line segment ensures the converges of the $F''(0, 0)$. In the similar way, one can investigate the so-called $\hbar$ curves of many other terms which have important physical meanings,

such as $F''(0, 1)$, $S''(0, 0)$, $S''(0, 1)$, $G'(0, 0)$, $G'(0, 1)$ and so on. Finally, one would find a region of $\hbar$ which ensures the convergence of all HAM solution series. For details, please refer to Liao [22] and others [25–40].

When $\xi = 0$, corresponding to the initial state, our analytic solutions agree well with the exact solutions (15), as shown in Fig. 1. When $\xi = 1$, corresponding to the steady-state, our analytic solutions agree well with the numerical solutions, as shown in Figs. 2–4. In additional, we have compared our sur-
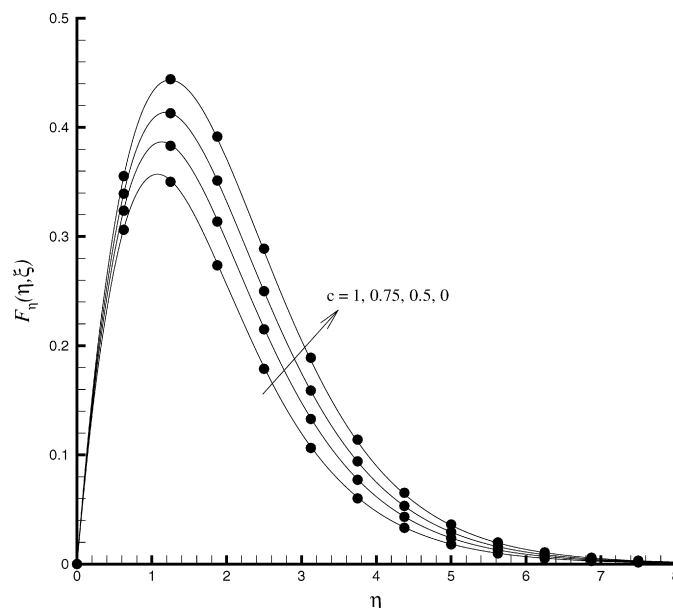

Fig. 2. The comparison of $F_\eta(\eta, \xi)$ of the analytic approximations with the numerical solutions at $\xi = 1$ for the different parameter c when $Pr = 0.72$. Filled circle: numerical solutions; Solid line: 25th-order HAM approximations for $\hbar = -1.5$.
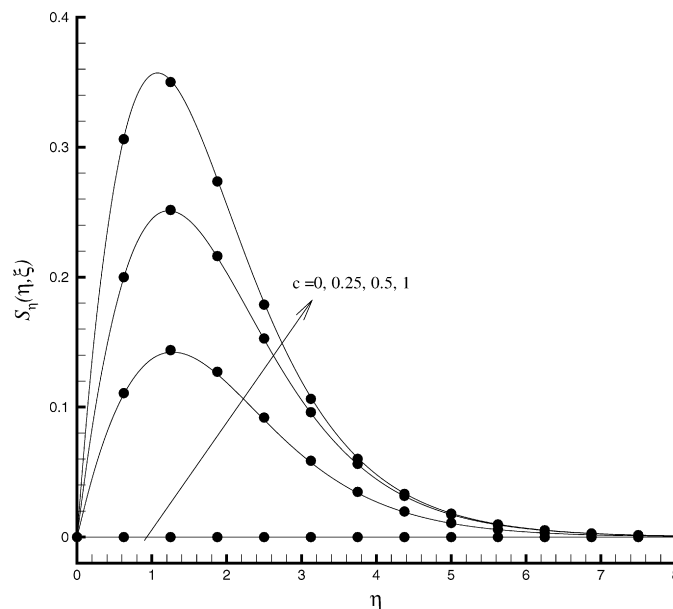
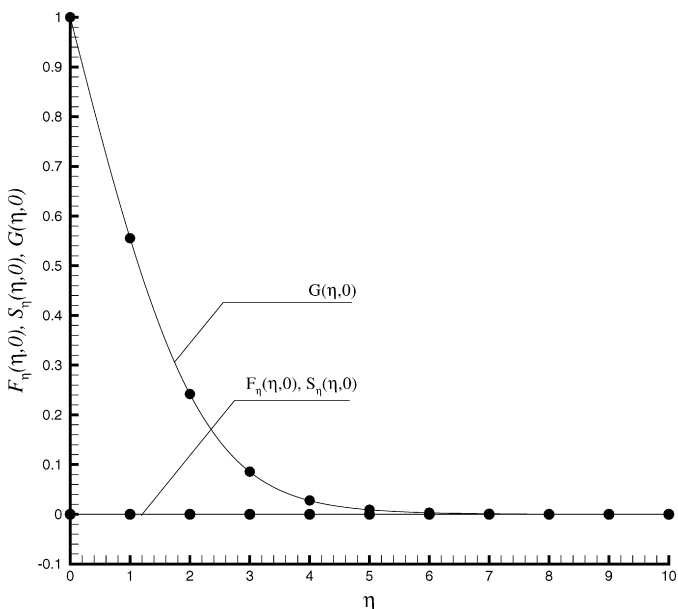

Fig. 1. The comparison of $F_\eta(\eta, \xi)$, $S_\eta(\eta, \xi)$ and $G(\eta, \xi)$ of the analytic approximations with the exact solutions at $\xi = 0$. Open circles: exact solutions; Solid line: 25th-order HAM approximations for $\hbar = -1.5$.

Fig. 3. The comparison of $S_\eta(\eta, \xi)$ of the analytic approximations with the numerical solutions at $\xi = 1$ for the different parameter c when $Pr = 0.72$. Filled circle: numerical solutions; Solid line: 25th-order HAM approximations $\hbar = -1.5$.
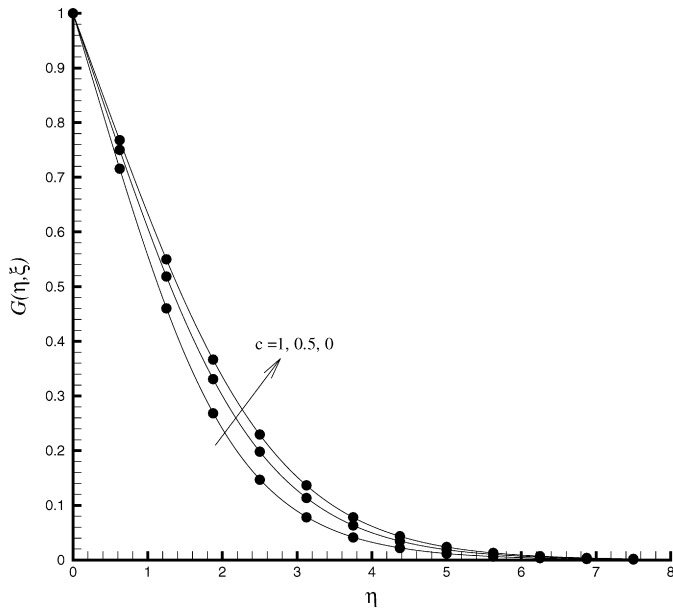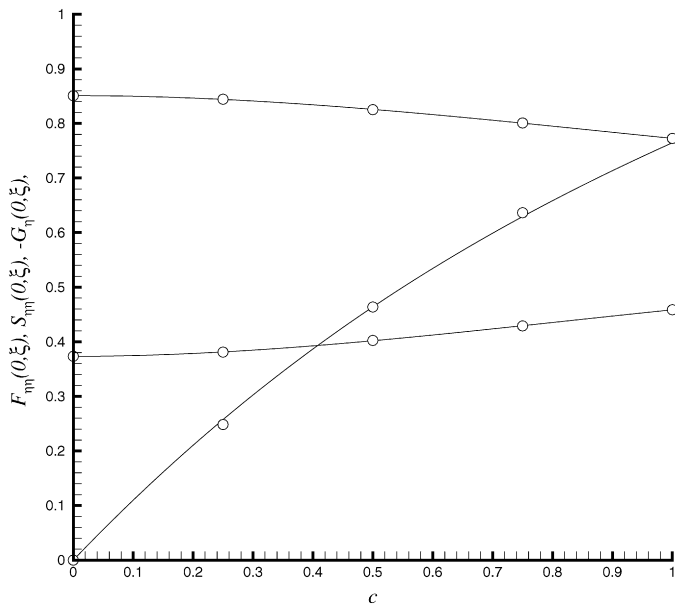
Fig. 4. The comparison of $G(\eta, \xi)$ of the analytic approximations with the numerical solutions at $\xi = 1$ for the different parameter c when $Pr = 0.72$. Filled circle: numerical solutions; Solid line: 25th-order HAM approximations $\hbar = -1.5$.

Fig. 6. The analytic approximations of $F_{\eta\eta}(0, \xi)$ for $0 \leqslant \xi \leqslant 1$ for different c when $Pr = 0.72$ and $\hbar = -1.5$. Solid line: 20th-order HAM approximations; Filled circles: 25th-order HAM approximations.

Fig. 5. The comparison of $F_{\eta\eta}(0, \xi)$, $S_{\eta\eta}(0, \xi)$ and $-G_\eta(0, \xi)$ of the analytic approximations with the Banks's results [5] at $\xi = 1$ for the different parameter c when $Pr = 0.72$. Open circle: Banks's results; Solid line: 25th-order HAM approximations $\hbar = -1.5$.

Fig. 7. The analytic approximations of $S_{\eta\eta}(0, \xi)$ for $0 \leqslant \xi \leqslant 1$ for different c when $Pr = 0.72$ and $\hbar = -1.5$. Solid line: 20th-order HAM approximations; Filled circles: 25th-order HAM approximations.

face skin friction and heat transfer results $F_{\eta\eta}(0, 1)$, $S_{\eta\eta}(0, 1)$ and $-G_\eta(0, 1)$ with those of Banks [5] and found them in excellent agreement, as shown in Fig. 5. These verify the validity of the proposed analytic approach. In a similar way, it is found that the solution series (33a)–(33c) are convergent in the whole range of the dimensionless time $\xi \in [0, 1]$, as shown in Figs. 6–8. Thus, by means of homotopy analysis method, we obtain analytic series solutions which are accurate and uni-
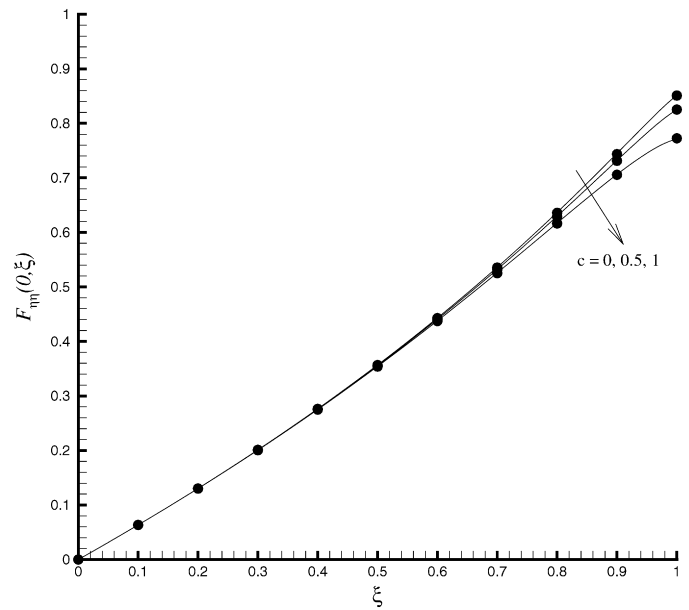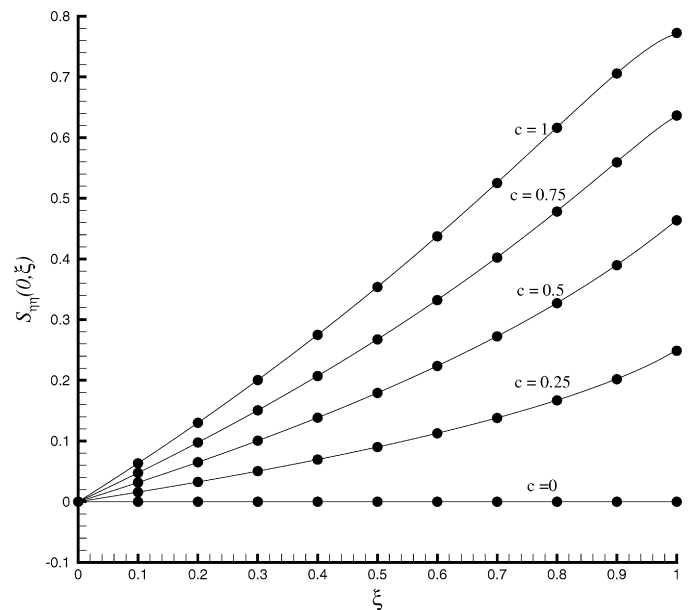
formly valid for all dimensionless time $\xi \in [0, 1]$ in the whole spatial region $0 \leqslant \eta < +\infty$. Such kind of solutions have not been reported, to the best of our knowledge.

The variation of the surface shear stresses in x- and y-directions and the surface heat transfer $F_{\eta\eta}(0, \xi)$, $F_{\eta\eta}(0, \xi)$, $-G_\eta(0, \xi)$ with dimensionless time ξ, for several values of c when $Pr = 0.72$, is drawn in Figs. 6–8. The surface shear stresses in x- and y-directions $F_{\eta\eta}(0, \xi)$, $G_{\eta\eta}(0, \xi)$ increase with ξ almost linearly. The surface heat transfer $-G_\eta(0, \xi)$ decreases with ξ for $\xi \leqslant \xi_0$ ($\xi_0 \approx 0.88$). Beyond this value, it
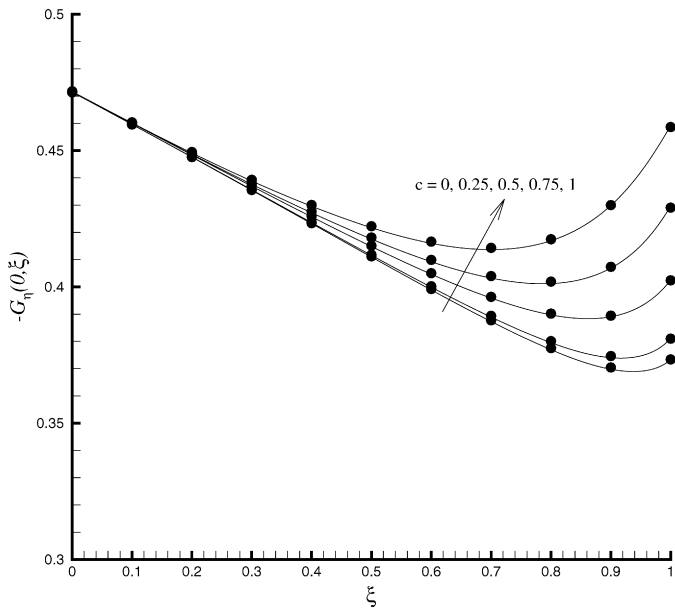
Fig. 8. The analytic approximations of $-G_\eta(0, \xi)$ for $0 \leqslant \xi \leqslant 1$ for different c when $Pr = 0.72$ and $\hbar = -1.5$. Solid line: 20th-order HAM approximations; Filled circles: 25th-order HAM approximations.
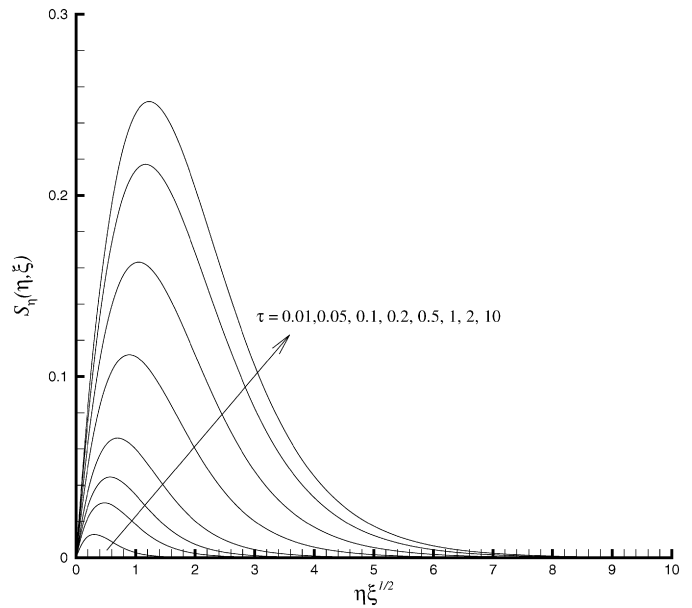

Fig. 10. The variation of the velocity profile $S_\eta(\eta, \xi)$ for $c = 0.5$ and $Pr = 0.72$ when $\hbar = -1.5$.
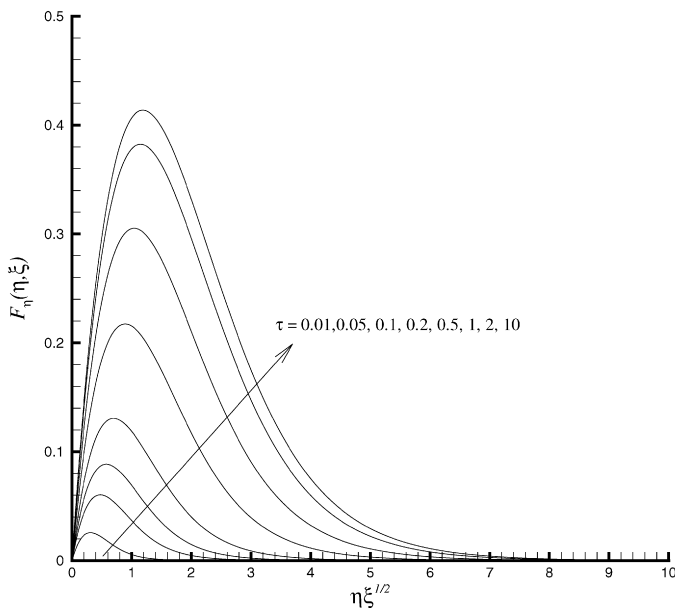

Fig. 9. The variation of the velocity profile $F_\eta(\eta, \xi)$ for $c = 0.5$ and $Pr = 0.72$ when $\hbar = -1.5$.
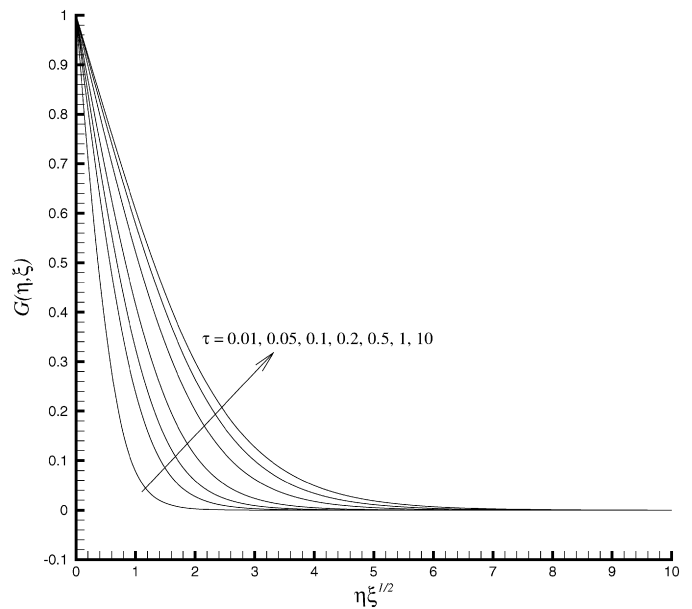

Fig. 11. The variation of the temperature profile $G(\eta, \xi)$ for $c = 0.5$ and $Pr = 0.72$ when $\hbar = -1.5$.

increases. The surface shear stresses in x-direction $F_{\eta\eta}(0, \xi)$ decrease as the parameter c increase, while the surface shear stresses in y-direction increase $S_{\eta\eta}(0, \xi)$ as the parameter c increase. The surface heat transfer $-G_\eta(0, \xi)$ also increase as the parameter c increases.

The development of the velocity profiles in the x- and y-directions $F_\eta(\eta, \xi)$, $S_\eta(\eta, \xi)$ and the temperature profiles $G(\eta, \xi)$ for $c = 0.5$ and $Pr = 0.72$ is shown in Figs. 9–11. We can see that these profiles develop rapidly from rest as τ increases from zero to ∞.

The curves of the local skin friction coefficients C_{fx} and C_{fy} versus τ for a fixed value of the parameter c when $Pr = 0.72$ are shown in Figs. 12 and 13, respectively. Note that, at the same dimensionless time $\tau \in (0, +\infty)$ and for the same Prandtl number Pr, the skin friction coefficient C_{fx} decreases as the values of the parameter c enlarges, while the skin friction coefficient C_{fy} increases as the values of the parameter c increase. The curves of the local Nusselt number Nu versus τ for a fixed value of the parameter c when $Pr = 0.72$ are shown in Figs. 14. Note that at the same dimensionless time $\tau \in (0, +\infty)$ and for the same Prandtl number Pr, the Nusselt number Nu decreases as the values of the parameter c enlarges.
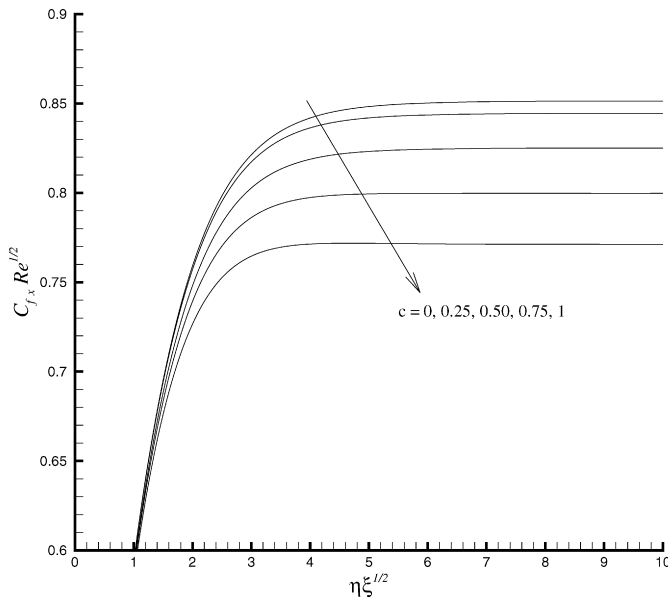
Fig. 12. The variation of the skin friction coefficient C_{fx} as a function of τ for the different parameter c when $Pr = 0.72$ and $\hbar = -1.5$.

Fig. 14. The variation of the Nusselt number Nu as a function of τ for the different parameter c when $Pr = 0.72$ and $\hbar = -1.5$.

used to investigate other similar nonlinear problems appeared in this field by the similar procedures.
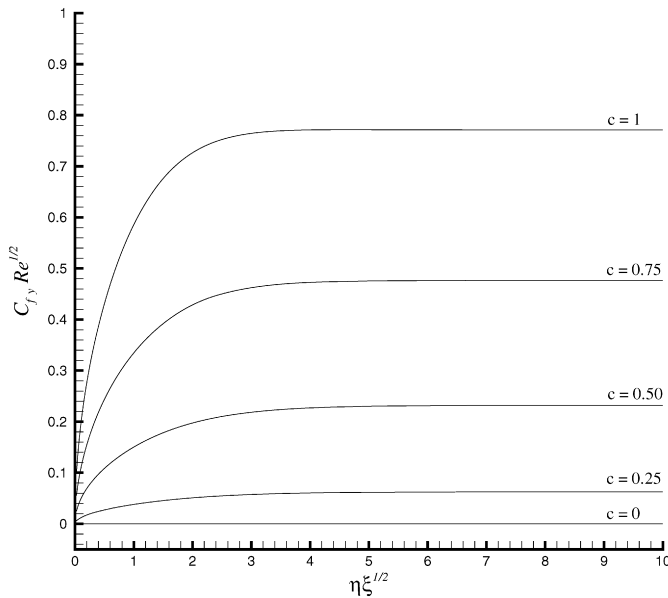
Fig. 13. The variation of the skin friction coefficient C_{fy} as a function of τ for the different parameter c when $Pr = 0.72$ and $\hbar = -1.5$.

5. Conclusions

In this paper, we have investigated the unsteady free convection flow in the stagnation-point region of a three-dimensional body in an ambient fluid. The original momentum and energy balance equations have been re-formulated by means of a set of new similarity transformations. Then the homotopy analysis method has been applied to obtain the accurate series solutions of the resulting equations. These solutions are valid for *all* dimensionless time $0 \leqslant \tau < \infty$ in the whole spatial region $0 \leqslant \eta < \infty$. It is expected that the similar similarity transformations can be used to other unsteady free convection problems. It is also expected that the proposed analytic technique can be
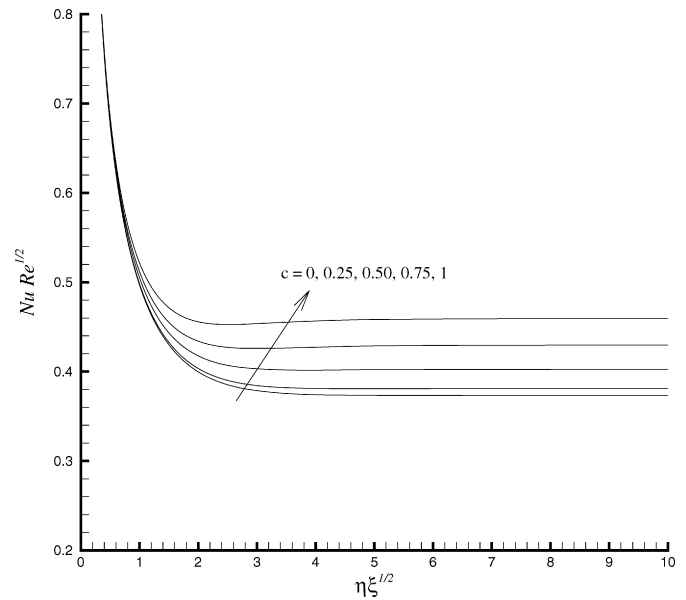
References

[1] A.J. Ede, Advances in free convection, Adv. Heat Transfer 4 (1967) 1–64.
[2] B. Gebhart, Natural convection flow and stability, Adv. Heat Transfer 9 (1973) 273–348.
[3] B. Gebhart, Y. Jaluria, R.L. Mahajan, R. Sammaria, Buoyancy Induced Flows and Transport, Hemisphere, New York, 1988.
[4] G. Poots, Laminar free convection near the lower stagnation point on an isothermal curved surface, Int. J. Heat Mass Transfer 7 (1964) 863–874.
[5] W.H.H. Banks, Laminar free convection flow at a stagnation point of attachment on an isothermal surface, J. Eng. Math. 8 (1974) 45–65.
[6] J.C. Williams, J.C. Mulligan, T.B. Rhyne, Semi-similar solutions for unsteady free-convection boundary layer flow on a vertical flat plate, J. Fluid Mech. 175 (1987) 309–332.
[7] H.S. Takhar, A. Slaouti, M. Kumari, G. Nath, Unsteady free convection flow in the stagnation-point region of a rotating sphere, Int. J. Non-Linear Mech. 33 (1998) 857–865.
[8] A. Slaouti, H.S. Takhar, G. Nath, Unsteady free convection flow in the stagnation-point region of a three-dimensional body, Int. J. Heat Mass Transfer 41 (1998) 3397–3408.
[9] J.H. Merkin, Free convection on a heated vertical plate: the solution for small Prandtl number, J. Eng. Math. 23 (1989) 273–282.
[10] V.P. Carey, Analysis of transient natural convection flow at high Prandtl number using a matched asymptotic expansion technique, Int. J. Heat Mass Transfer 26 (1983) 911–919.

[11] J.H. Merkin, T. Mahmood, On the free convection boundary layer on a vertical plate with prescribed surface heat flux, J. Eng. Math. 24 (1990) 95–107.

[12] M. Kumari, A. Slaouti, H.S. Takhar, S. Nakamura, G. Nath, Unsteady free convection flow over a continuous moving vertical surface, Acta Mech. 116 (1996) 75–82.

[13] M. Miyamoto, Influence of variable properties upon transient and steady-state free convection, Int. J. Heat Mass Transfer 20 (1977) 1258–1261.

[14] V.M. Soundalgekar, P. Ganesan, Transient free convection with mass transfer on a vertical plate with constant heat flux, Int. J. Energy Res. 9 (1985) 1–18.

[15] P. Cheng, Free convection about a vertical flat plate embedded in a porous medium with application to heat transfer from a dike, J. Geophysical Res. 82 (1977) 2040–2044.

[16] K. Aziz, J.D. Hellums, Numerical solution of the three dimensional equations of motion for laminar natural convection, Phys. Fluid 10 (1967) 315–324.

[17] W.H.H. Banks, Three-dimensional free convection near a two-dimensional isothermal surface, J. Eng. Math. 6 (1972) 109–115.

[18] A. Suwono, Laminar free convection boundary layer in three-dimensional system, Int. J. Heat Mass Transfer 23 (1980) 53–61.

[19] H. Xu, An explicit analytic solution for free convection about a vertical flat plate embedded in a porous medium by means of homotopy analysis method, Appl. Math. Comput. 158 (2004) 433–443.

[20] C. Wang, S.J. Liao, J.M. Zhu, An explicit solution for the combined heat and mass transfer by natural convection from a vertical wall in a non-Darcy porous medium, Int. J. Heat Mass Transfer 46 (2003) 4813–4822.

[21] S.J. Liao, The proposed homotopy analysis technique for the solution of nonlinear problems, PhD thesis, Shanghai Jiao Tong University, 1992.

[22] S.J. Liao, Beyond Perturbation: Introduction to the Homotopy Analysis Method, Chapman & Hall/CRC Press, Boca Raton, 2003.

[23] S.J. Liao, An explicit, totally analytic approximation of Blasius viscous flow problems, Int. J. Non-Linear Mech. 34 (1999) 759–778.

[24] S.J. Liao, Series solutions of unsteady boundary-layer flows over a stretching flat plate, Stud. Appl. Math. 117 (2006) 2529–2539.

[25] T. Hayat, M. Sajid, On analytic solution for thin film flow of a fourth grade fluid down a vertical cylinder, Phys. Lett. A 361 (2007) 316–322.

[26] M. Sajid, T. Hayat, S. Asghar, Comparison between the HAM and HPM solutions of thin film flows of non-Newtonian fluids on a moving belt, Nonlinear Dyn., in press.

[27] S. Abbasbandy, The application of the homotopy analysis method to nonlinear equations arising in heat transfer, Phys. Lett. A 360 (2006) 109–113.

[28] S. Abbasbandy, The application of the homotopy analysis method to solve a generalized Hirota–Satsuma coupled KdV equation, Phys. Lett. A 361 (2007) 478–483.

[29] Y. Song, L.C. Zheng, X.X. Zhang, On the homotopy analysis method for solving the boundary layer flow problem over a stretching surface with suction and injection, J. Univ. Sci. Tech. Beijing 28 (2006) 782–784 (in Chinese).

[30] Y.R. Shi, J.X. Xu, Z.X. Wu, Application of the homotopy analysis method to solving nonlinear evolution equations, Acta Phys. Sinica 55 (2006) 1555–1560 (in Chinese).

[31] S. Asghar, M.M. Gulzar, M. Ayub, Effect of partial slip on flow of a third grade fluid, Acta Mech. Sinica 22 (2006) 195–198.

[32] T. Hayat, M. Sajid, Analytic solution for axisymmetric flow and heat transfer of a second grade fluid past a stretching sheet, Int. J. Heat Mass Transfer 50 (2007) 75–84.

[33] T. Hayat, Z. Abbas, M. Sajid, S. Asghar, The influence of thermal radiation on MHD flow of a second grade fluid, Int. J. Heat Mass Transfer 50 (2007) 931–941.

[34] T. Hayat, M. Khan, Homotopy solutions for a generalized second grade fluid past a porous plate, Nonlinear Dyn. 42 (2005) 395–405.

[35] M. Sajid, T. Hayat, S. Asghar, On the analytic solution of the steady flow of a fourth grade fluid, Phys. Lett. A 355 (2006) 18–26.

[36] Z. Abbas, M. Sajid, T. Hayat, MHD boundary-layer flow of an upper-convected Maxwell fluid in a porous channel, Theor. Comput. Fluid Dyn. 20 (2006) 229–238.

[37] S.P. Zhu, A closed-form analytical solution for the valuation of convertible bonds with constant dividend yield, Anziam J. 47 (2006) 477–494.

[38] S.P. Zhu, An exact and explicit solution for the valuation of American put options, Quant. Finance 6 (2006) 229–242.

[39] M. Ayub, A. Rasheed, T. Hayat, Exact flow of a third grade fluid past a porous plate using homotopy analysis method, Int. J. Eng. Sci. 41 (2003) 2091–2103.

[40] T. Hayat, M. Khan, M. Ayub, On the explicit analytic solutions of an Oldroyd 6-constant fluid, Int. J. Eng. Sci. 42 (2004) 123–135.

[41] J.H. He, Homotopy perturbation technique, Comput. Methods Appl. Mech. Eng. 178 (1999) 257–262.

[42] J.C. Williams, T.H. Rhyne, Boundary layer development on a wedge impulsively set into motion, SIAM J. Appl. Math. 38 (1980) 215–224.